Available online www.jsaer.com

***Journal of Scientific and Engineering Research*, 2021, 8(5):118-131**

Research Article

ISSN: 2394-2630
CODEN(USA): JSERBR

Modeling of the Magnetic Behavior of Ferromagnetic Materials in Transformers

Gaskel Gning[1, 2], Dianguina Diarisso[1], Oumar Diallo[1], Mamadou Sall[3], Jean Jacques Rousseau[2]

[1]LM3E, Electrical Engineering and Computer Science, IUT/University of Thies, Thies, Senegal
[2]Laboratoire Hubert Curien (LabHC) Saint-Etienne, France

Abstract Magnetic materials are basic components of electromagnetic systems, the behavior of which must be controlled more and more in order to meet economic, environmental and operational safety constraints.
These systems, especially transformers and inductors, are based on a transfer of magnetic energy.
Magnetic materials, present in these systems, are at the heart of energy conversion and must be optimized to achieve efficient energy conversion.
Thus in addition to the working frequency which can vary, the materials are subjected to very diverse waveforms which are imposed by the power supply but also generated by the saturation of the materials, the geometry of the magnetic circuit, the magnets, the leaks, etc.

Keywords Imodeling, Ferromagnetic Materials, Transformers

1. Introduction

In electrical machines, for example, materials are subjected to extreme stresses which are very different from the usual or standardized characterization conditions. The standard characteristics are then insufficient to predict the behavior of the magnetic circuit, and the prior evaluation of the iron losses therefore remains today a delicate problem that the manufacturers of electrical devices bypass by using empirical corrective factors.
For these ferromagnetic materials, it is therefore necessary to have models of hysteretic behavior in any static and dynamic regimes (permanent and transient) in order to optimize the operation of electromagnetic systems, and in particular, to predict waveforms and losses. The explanation, control and modeling of the behavior of ferromagnetic materials are still relevant today.
The objective of this work is the transformer in the time domain. For this, we will first present the main models that exist in the literature and their characteristics.
Automatic section, CFPT, Dakar, Senegal
In order to choose a model presenting possible improvements on the modeling of the transformer to determine a model which simulates as closely as possible the behavior of the transformer studied.

2. MAGNETISM IN MATTER

2.1 Phenomenology

Magnetic materials occupy a very large place in technology, and their applications are very numerous.
The magnetic state of matter can be characterized by a vector $\vec{M}$ called magnetization, or dipole magnetic moment per unit volume. In a vacuum, the magnetic field $\vec{B}$ and the magnetic excitation $\vec{H}$ are related by the relation: $\vec{B} = \mu 0\vec{H}$ where $\mu 0 = 4\pi \cdot 10{-}7$ VsAm is the absolute permeability of the vacuum. On the other hand,

in matter, the magnetic field depends on the magnetization $\vec{M}$ of the matter in the following way: $\vec{B} = \mu o\vec{H} + \vec{M}$ [1]

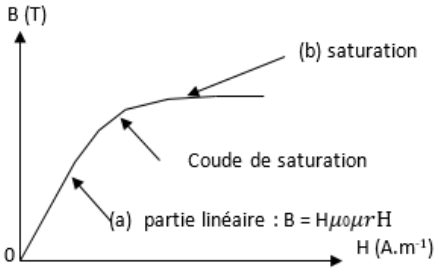

The magnetization $\vec{M}$ of matter is a function of the excitation $\vec{H}$, of the nature of the substance, and of the magnetic, mechanical and thermal treatments previously undergone by the substance.

The figure opposite shows the general shape of the dependence curve of B as a function of H in matter.

This curve shows that the induction B tends towards a limit value Bs called the saturation value. There are two areas:

a linear zone (a) and a saturation zone (b). In the linear zone ($H<Hs$), we can write: $\vec{M} = \mu 0\chi m\vec{H}$ where χm is the magnetic susceptibility of the sample of matter considered. It follows that: $\vec{B} = \mu 0\vec{H}\ (\chi m + 1) = \mu 0\mu r\vec{H}$ where $\mu r = \chi m + 1$ is the relative permeability of the material considered

In the saturation zone ($H>Hs$), $\vec{M}$ is no longer a linear function of $\vec{H}$. We can therefore no longer write $\vec{B} = \mu 0\mu r\vec{H}$, because μr would no longer be a constant, but a function of $\vec{H}$. [1]

2.2 Cycle hystérésis

The hysteresis cycle illustrates the relationship between the magnetization $\vec{M}$ (or the field $\vec{B}$) as a function of the applied magnetic excitation $\vec{H}$.

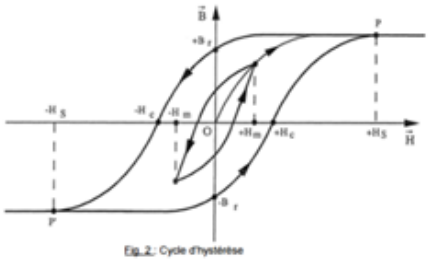

It characterizes each ferromagnetic body and its shape depends on the geometry of the sample, the mechanical stresses to which the latter is subjected, its temperature, etc. We can distinguish: - the first magnetization OP curve - the value Hs of the saturation field. - the value Br of the remanent induction - the value Hc of the coercive field - the symmetry of the cycle (points P '($-Hs$) and P (Hs) with respect to O).

If we make the field H oscillate between two limits $-Hm$ and Hm, symmetrical with respect to O, with $Hs \neq Hm$, we obtain other cycles which still admit the origin O as center of symmetry. The course of a cycle of hysteresis under the effect of a cyclic external magnetic field dissipates energy within the ferromagnetic material [2].

3. The Transformer in Sinusoidal Regime

3.1. Definition

A transformer is a quadrupole formed of two windings encircling a common magnetic circuit. It is a static machine allowing, in alternating mode, the modification of certain quantities (voltage, current) without changing their frequency

3.2 Constitution

The transformer is a static converter which converts an alternating signal into another alternating signal of the same frequency but of different rms values. It is either voltage or current step-up or step-down. It can also be used as an insulating element between two circuits [3] It is made up of:

- A magnetic circuit in soft and laminated ferromagnetic material (to limit iron losses)
- A coil of N1 turns supplied by the network (PRIMARY)

A coil of N2 turns which supplies a voltage to the load (SECONDARY)

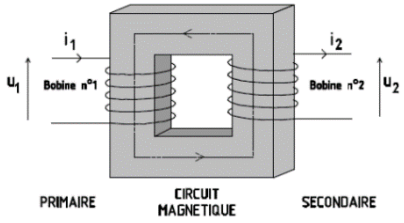

3.2.1 Magnetic circuit: The magnetic circuit of the transformer consists of several ferromagnetic sheets in the shape of "E" and "I" "head-to-tail" assemblies. If it is crossed by a variable magnetic field, it exhibits saturation phenomena, eddy current losses and hysteresis losses [3].

3.2.2 Windings: The magnetic circuit has 2 coils (single-phase) whose number of turns are respectively N1 and N2.The notation of the sizes of the primary coil is noted by index 1. Regarding the sizes of the secondary coil, they are noted by index 2. The coil which is supplied is called "primary coil", and the other coil is called the "secondary coil". The primary and secondary windings are wound in the center, in the same direction, primary on the inside and secondary on the outside.

3.3 Energy balance: The efficiency (ŋ = P2 / P1 <1) shows the existence of losses at the level of the transformer because its useful power (P2) is always lower than its power absorbed at the primary (P1) [3]

3.3.1 Losses by Joule effect or losses in copper the primary and secondary windings have resistances denoted by R1 and R2. The transformer will therefore be the site of losses by the Joule effect (also called copper losses) respectively by the effect of the currents I_1 and I_2 **:** $\boldsymbol{C = R_1 I_1^2 + R_2 I_2^2}$ [4].

3.3.2 Magnetic losses or losses in iron

3.3.2.1 Losses by hysteresis: The magnetization of the material absorbs energy. As the phenomenon is not reversible, the material does not restore all the energy received. During demagnetization, part of it dissipates in the form of heat. These losses are proportional to the area of the hysteresis cycle (figure opposite) [4].

3.3.3 Advanced model

Classically, the previous equivalent diagram is constructed from resistive and inductive elements assumed to be constant, but they can vary as a function of frequency and time. Indeed, in steady state, transformers operate in a so-called linear zone where magnetization requires only little power (little magnetomotive force, little current). On the other hand, some regimes request a zone beyond the linear zone, called the saturated zone, where the limits of the ferromagnetic material are reached where magnetization requires much more power (current). Thus, the magnitude of the magnetizing current can reach in a saturated zone (while the transformer is empty) several times that of the nominal current. The saturation characteristic given by a curve of the flux in the core as a function of the magnetizing current is represented by a non-linear inductance Lm The curve of the flux in the core as a function of the magnetizing current φ (Im) is represented by a simplified model of the figure below with Lm its slope in linear zone and Ls its slope in saturated zone [6].

3.4 Nonlinear model

3.4.1 Introduction

Many authors have been interested in taking into account the nonlinearity of magnetic components (hysteresis, saturation and eddy currents).This approach allows a more precise improvement regardless of the waveform and allows to calculate the losses in the magnetic material. The most popular model is the Jiles and Atherton model, which is found in a large number of simulators (Spice, EMTP ...). Thus, a variety of methods for transformer modeling have been developed for decades and among these models we present the Jiles-Atherton models in more detail.

3.4.2 History

The main objective of the various models encountered in the literature is to mathematically approach the phenomenon of hysteresis or at least, its representative curve. The major difficulties of interpretation of the phenomenon result from the fact that it is not a physical property of the material but involving several parameters and at different scales. The experiment shows the effect of parameters such as: frequency,

temperature, intensity of the excitation field, etc .The main quantities representing the hysteresis are (H) and (M) which are by nature vector quantities. All the representations should then normally generate vector quantities. However, several theoretical approaches and measurement methods are based on a scalar representation which gives the components (M) or (B) according to the field modulus (H).The scalar description of the phenomenon may be satisfactory in several study cases even if the sample has a favored direction of magnetization [6].

3.4.3 State of the art on types of models

There are a large number of models of the static behavior of magnetic materials. We can cite non-analytical models, such as distribution function models, the most famous and widely used of which is the Preisach model (Preisach, 1935). Next, analytical models such as those of Rayleigh (Ponomarev, 2008) or Frohlich (Frohlich, 1881) (Kennelly, 1891) (Bozorth, 1951), very attractive by their simplicity of implementation and widely used in the codes ofcalculation but these models have no physical consideration and only develop a function between H and B. And finally more complex analytical models, such as the Jiles-Atherton model (Jiles, et al. 1984) (Jiles, 1990) (Jiles, et al. 1992). These models develop a function between B and H from physical and energetic considerations.¬ [6].

3.4.4 The Rayleigh model Rayleigh'smodel (Rayleigh (Lord), 1887) is one of the oldest analytical models. It is only used for weak fields, outside the saturation zone. It expresses the magnetic flux density as a function of the magnetic field as a second order polynomial. Thus, for a magnetic field varying between −Hmax and + Hmax, the magnetic flux density is worth:

$$\mathbf{B} = (\mu_{initial} + \eta.\mathrm{Hmax}).H + \mathrm{sgn}(dH).\frac{\eta}{2}.(H^2 - Hmax^2)$$

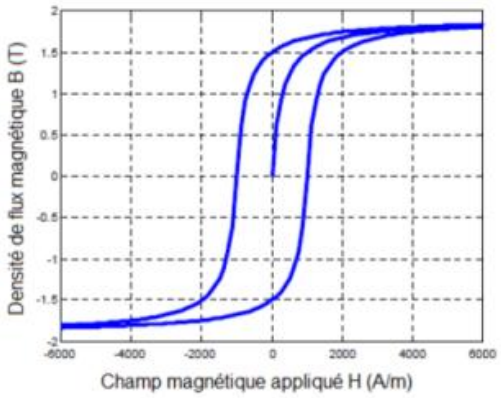

$\mu initial$ is the initial permeability, Hmax the maximum excitation, η the Rayleigh constant. The Rayleigh constant represents the irreversible effects of the phenomenon of magnetization. The mathematical function sign ≪sgn≫ is defined by $\mathrm{Sgn}(\chi) = \begin{cases} +1 \; si \; x > 0 \\ -1 \; si \; x < 0 \\ 0 \; sinon \end{cases}$

The shape of a hysteresis cycle modeled by the Rayleigh equations is represented by the figure below Typical cycle modeled by Rayleigh NB: For this model, the general pace of the cycle and especially of the range is limited

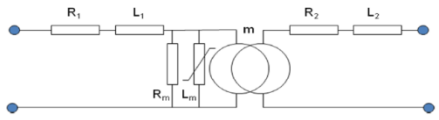

3.4.5 The Frohlich model

This model describes the curve of first magnetization, and therefore this model is initially anhysteretic. It was improved by the works of Akbaba (Akbaba, 1991).The Frohlich model is defined by the relations:

$$\mathbf{B} = \frac{(H - sgn(dH).Hc)}{\alpha + \beta.|H - sgn(dH).Hc|}$$

With $\alpha = Hc\left(\frac{1}{Br} - \frac{1}{Bs}\right)$ and $\beta = \frac{1}{Bs}$

Where α and β are the parameters of the Frohlich model, Hc the coercive field, Br the remanent induction and Bs the saturation induction. The shape of a hysteresis cycle modeled by Frohlich's equations is shown below: [6] Typical cycle modeled by Frohlich NB: This model cannot accurately represent the piecewise linear shape of the cycle of nanocrystalline materials.

3.4.6 Preisach model: The approach of this scalar model developed in 1935 by the German physicist Preisach is completely intuitive and is based on an understanding of the mechanism of magnetization. The Preisach model is based on two fundamental notions, namely: ¬ The rectangular elementary hysteresis cycle called "Hystéron" which physically represents a Weiss domain which is magnetized to saturation; ¬the distribution density function of the hystons known as the "distribution function" which represents the distribution of Weiss domains in a ferromagnetic material. The magnetic state of the material described by this set of magnetic entities (hystons) has two possible saturation states (M = ± 1). These hystons are each represented by a rectangular elementary cycle offset from the origin. [6] Each of these hystons behaves like a simple hysteresis comparator, asymmetric with respect to the origin

Thus, thanks to the knowledge of a distribution function of these elementary cycles, called the Preisach distribution function, we can calculate the magnetization at any time

$$\mathbf{M(t) = \iint \rho(\alpha,\beta).\Phi\alpha\beta[H(t)]d\alpha\, d\beta}$$

Where ρ (α, β) is the Preisach distribution function and Φαβ [H (t)] is the mathematical operator associated with the hysteron and takes the value +1 or -1 depending on the direction of variation of the magnetic field andthe value of the field compared to the toggle field (see Figure above).

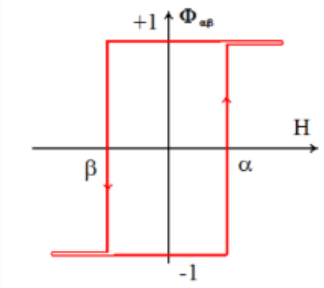

NB: This model leads to powerful results which have been supported by numerous implementations but requires a lot of experimental data to establish the distribution function.The Preisach scalar model makes it possible to calculate the magnetization depending on the values of the applied excitation field..The only handicap as to its use lies in the determination of its distribution function. [6]

3.4.7. Preisach-Bertotti (1994)

Originally, the Preisach model of hysteresis generalized magnetic hysteresis as a relationship between the magnetic field and the magnetization of a magnetic material such as the parallel connection of independent relay hysterons.In the field of ferromagnetism, it is sometimes thought that the Preisach model describes a ferromagnetic material as a network of small, independently acting domains.An iron sample, for example, can have magnetic domains evenly distributed, resulting in a net magnetic moment of zero.

A mathematically similar model appears to have been developed independently in other fields of science and engineering. A notable example is the model of capillary hysteresis in porous materials developed by Everett and his colleagues. Since then, after the work of people like M. Krasnoselkii, A. Pokrovskii, A. Visintin and ID Mayergoyz, the model has become

Widely accepted as a general mathematical tool for the description of hysteresis phenomena ssof various types. G. Bertotti, V. Basso and M. Pasquale propose in 1994 a dynamic generalization of the statistical computation of Preisach on a set of commutators.

This dynamic can integrate any type of magnetization process, including the main mechanism which is the displacement of the magnetic walls. This adaptation is done by attributing to the switches γ_ (a, b) of the following figure a dynamic law of change of state which depends on the time derivative of the elementary flow of each of them, hence the introduction of a new parameter k linked to the mobility of the magnetic walls. [6]

3.4.8 Jiles - Atherton Model

3.4.8.1 Mathematical formulation of the model: The Jiles-Atherton model, introduced in 1983, is a model that describes the origin of the phenomenon of hysteresis in ferromagnetic materials from a physical approach. This description is based on energy considerations linked to the movements of walls within the magnetic system. It is widely used to model the nonlinear characteristics of magnetic hysteresis.

Initially, the Jiles-Atherton model is a hysteresis model based on Langevin's theory, corrected by Weiss theory. The authors of the model refined this physical basis to take into account irreversible changes in magnetization, caused in particular by wall movements [6].

In their work, the authors assume that the total magnetization M of the material is the superposition of a reversible component M_rev representing the reversible movements of the walls of the magnetic domains defined by Weiss and of an irreversible component M_irr grouping the non-reversible movements of these walls. Both obeying differential relationships built from an anhysteretic magnetization M_an of Langevin and an effective field H_e damped by the mean field of Weiss αM (H_e = H + αM) M = M_rev + M_irr The relation between these two components and the anhysteretic magnetization is obtained from physical considerations of the magnetization process and is given by:

$$\boldsymbol{M_{rev}} = \mathbf{c}.(\boldsymbol{M_{an}} - \boldsymbol{M_{irr}})$$

$$M_{an} = M_S .\left(Coth\left(\frac{H_e}{\mathrm{a}}\right) - \frac{\mathrm{a}}{H_e}\right)$$

$$\frac{\boldsymbol{dM_{irr}}}{\boldsymbol{dH_e}} = \frac{(\boldsymbol{M_{an}} - \boldsymbol{M_{irr}})}{(\boldsymbol{k.sgn}\,(\boldsymbol{dH}))}$$

$$H_e = \mathrm{H} + \alpha.\mathrm{M}$$

$$\mathrm{B} = \mu_0(H + M)$$

Where: a, c, 〖k, α, and the saturation magnetization M〗 _S are the 5 Jiles parameters which are determined from the measured hysteresis characteristics.

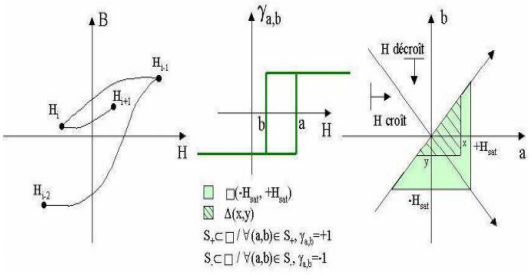

Explanatory diagram of the switches and the Preisach plan

3.4.8.2 Parameters of the Jiles-Atherton model

According to the authors of the model, these parameters have the following physical meaning:

χ_{ini} and χ_{an} are the initial normal and anhysteretic differential susceptibilities;

χ_c :Differential susceptibility at the coercive point;

Hc:coercive field

The determination of these parameters requires knowledge of experimental data such as the major cycle, the curve of first magnetization as well as the anhysteretic curve. [7]

3.3.8.2.1 Parameter a

It characterizes the variation of anhysteretic magnetization as a function of the effective field. The following figures show that a decrease in the parameter a results in an increase in the maximum induction Bs, in the remanent induction Br and a slight decrease in the coercive field Hc. This means that this parameter determines the degree of inclination.

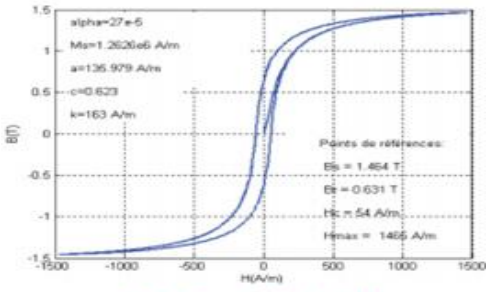

Cycle d'hystérésis de référence

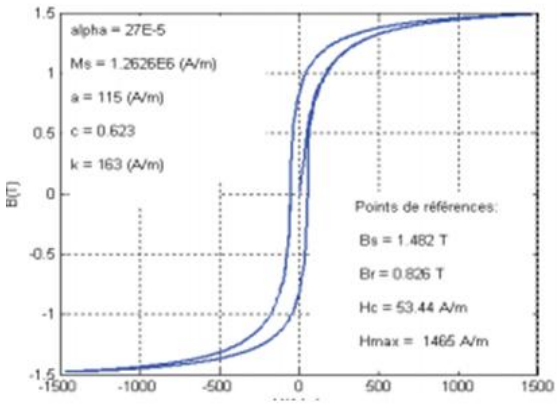

Reference hysteresis cycle

3.4.8.2.2 Parameter c

It characterizes the process of reversibility of magnetization. The figures below show that a decrease in this parameter results in a slight decrease in Bs, an increase in Br and Hc. This can be explained by the low rate of reversible magnetization compared to irreversible magnetization.

Paramètre		Propriété physique	Formulation mathématique
c		Coefficient de réversibilité	$\frac{3a\chi_{ini}}{M_s}$
a	A/m	Facteur de forme pour *M an*	$\frac{M_s}{3}\left(\frac{1}{\chi_{an}}+\alpha\right)$
k	A/m	Facteur lié aux pertes par hystérésis	$\frac{M_{an(H_c)}}{1-c}\left[\alpha+\frac{1}{\frac{1}{1-c}\chi_c-\frac{c}{1-c}\frac{dM_{an}(H_c)}{dH}}\right]$
α		Lié à l'interaction entre domaines	Obtenu à partir de l'équation donnant l'aimantation rémanente *Mr*
Ms	A/m	Aimantation de saturation	Obtenue à partir du cycle majeur.

Effect of parameter c

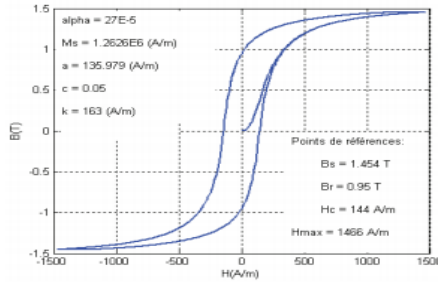

3.4.8.2.3 Parameter k

It characterizes the width of the cycle (figures below) Hc and Br decrease sharply when this parameter decreases.

3.4.8.2.4 Parameter α

It corresponds to the coupling between magnetic moments (figures below). When its value decreases, it brings about a decrease in Bs, Br and Hc.

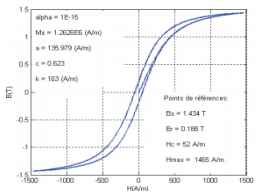

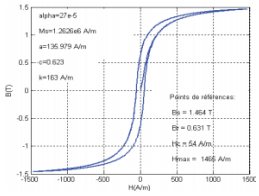

Cycle d'hystérésis de référence **Effet du paramètre α**

3.4.8.2.5 Ms Parameter

The decrease in saturation results in a decrease in Br and Hc (figures below).

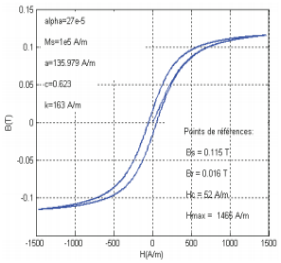

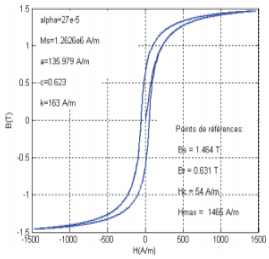

NB: The parameters of the model are interdependent, the variation of one of them causing variation of the others. The cycle is very sensitive to the variation of its parameters.

Effet du paramètre Ms Cycle d'hystérésis de référence

3.4.8.3 Criticism of the Jiles-Atherton model

The J-A model does not reproduce sufficiently the shape of the magnetic hysteresis curve near the saturation state

The minor hysteresis curves reproduced by the J-A model are generally asymmetrical and do not form a closed curve, however, the model has consistently eliminated or at least minimized its defects. The two most glaring (and annoying) imperfections are (M. Marion Romain):

The variation of the parameters as a function of the maximum field value applied for certain families of materials as shown in the following Figure. For this figure, the measurements were carried out on FeSi GNO sheets 0.5 mm thick.

The non-congruence of minor cycles: After a reversal of the applied field and a return to its value before reversal, the induction value is no longer the same and thus the cycles do not "close" to the point of first rollover (Figure below)

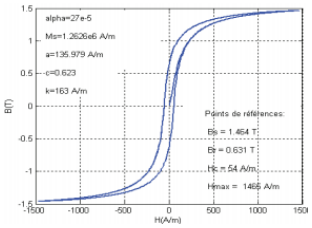

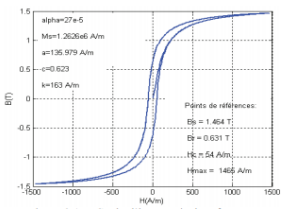

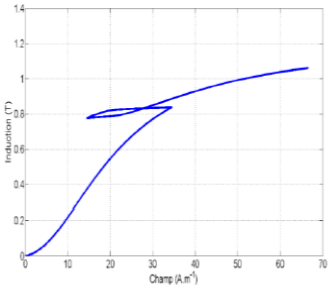

Cycle d'hystérésis de référence Effet du paramètre k

Figure III-20 : Mise en évidence de la non-congruence du modèle lors d'une boucle mineure

3.4.9. Conclusion

In this first part of the chapter, we are mainly interested in the hysteresis cycle which represents a behavior nonlinear ferromagnetic materials, hence the need for an efficient physical model. Several models are reported in the most used literature are mainly the Preisach model and the Jiles-Atherton model. These two models are based on the physics of ferromagnetic materials

4. The Other Modeling

The universal EMTP model

The universal calculation code EMTP (Electromagnetic Transients Program) is used to study the behavior of electrical networks, in transient regime. It is used as a standard in time and frequency studies. The use of this calculation code to model a transformer consists in representing the latter by an equivalent electrical diagram, comprising:

- perfect transformers;
- asaturable magnetizing branch modeling the iron core;
- group leakage inductors (wafers, layers, or coils);
- And finally, resistance of the windings, and coupling capacities. The different parameters of the equivalent diagram shown in Figure 1 (R1 resistance of the wafer 1,) are determined, either by numerical or analytical calculation, from the geometry of the transformer, and by making simplifying assumptions (symmetry, permeability of the core constant magnetic,), either by measurement (no-load tests, short-circuit tests, ...) [8].

The main advantage of using the EMTP model is that one can carry out interaction studies of the transformer, with the network, in quasi-real configurations (presence of protections,). Indeed, in addition to the linear elements (linear resistances and inductances), it also treats the nonlinear elements, such as the surge arresters.

But, in some cases, the use of the EMTP calculation code, to model a transformer, does not represent reality. Indeed**,**

for example for a single-phase transformer with two equal windings (high voltage and low voltage), the EMTP model is not symmetrical, and the short-circuit inductance is not the same, seen from the primary and the secondary (Figure 2).

Finally, the studies we have done show the field of use of the EMTP model: it is well suited for studies of networks (with a global modeling of the transformer), but it is not suitable for internal studies of the transformer. The models presented below are present in the literature, but do not attract researchers in Electrical Engineering so much, because they have a fairly specific and restricted field of validity [8].

4.1. Modeling by modal analysis

Modal analysis is a method used to describe a system that can oscillate, using modal parameters, which are obtained from measurements.

The modeling of a transformer by modal analysis consists in considering it as a black box (quadrupole), and we are interested in the waveforms at its ends (input and output). The output signal being linked to the input signal via the transfer function, when an excitation voltage (maneuver waves or lightning strikes) contains one of the natural frequencies of the transformer, this results in resonance excitation. , and the transformer becomes the seat of oscillations. The general principle of this method is as follows: at each frequency, from the measurements of the input current I, and of the input voltage Ve of the transformer, and making the ratio L / Ve, the evolution of its this curve (natural form, natural frequency, and damping), we obtain the equivalent circuit, as well as the resonant frequencies of the transformer.

An in-depth study of the oscillatory behavior of power transformers, from modal analysis, shows the interest of this approach. Similarly, much more developed models for the calculation of transmitted voltages show its strong point for network studies: modeling by modal analysis allows on the one hand the calculation of resonance frequencies, with good precision, and on the other hand it gives a suitable equivalent diagram, for taking into account the reaction on the network of a transformer.

But, this method has a major drawback: to apply it, it is necessary to have made series of measurements, and consequently the reliability of the final model depends on the precision of results of these latter.

Choice between the time approach and the frequency approach

The calculation codes intended for modeling power transformers have developed in two parallel ways: the first is a solution in the time domain, and the second a solution in the frequency domain. If the model is linear and lossless, the two methods are equivalent.

The requirement for a voltage response in the time domain is based on the need to design the structure of the transformer insulation. Furthermore, a solution in the time domain represents a considerable advantage when we

consider non-linear elements such as the magnetic core and metallic oxide devices, or when we consider modifications in the topology of the model (for example the closure or the 'opening of a switch). The equivalent network corresponding to this approach leads to a Foster or other type circuit, where there is an association of several dipoles, which increase the size of the network, therefore the resolution time (calculation).
In addition, the frequency domain solution represents clear advantages if we consider the variable losses with the waveform, which are created in the windings, in the dielectrics, and in the core of a transformer (the latter solution does not allow us to take into account the presence of non-linear elements, unlike the first).

5. Conclusion

We have seen in this bibliographical study the various models of high frequency power transformer, existing in the literature. The model R, L, C based on the own, mutual, and leakage inductances is the most suitable for our work, and therefore used to study the behavior of power transformers, in transient regime (calculation of resonance frequencies and coefficients of overvoltage).
Up to now, phenomena such as the additional eddy current losses, the behavior of the magnetic core, and the dielectric losses, are approximated, or quite simply neglected, because their calculations, using numerical methods, are expensive in calculation time.
For our study, we adopt the frequency approach which can give us the resonance frequencies and the corresponding overvoltage factors. However, with this choice, a compromise between precision and computation time is imperative, because at each frequency we must solve the same network (equivalent scheme). This is why we will calculate in an analytical way the parameters resistances and inductances of the equivalent diagram of the transformer. Using an FFT, we will be able to obtain the answers in the time domain of the transformer, information which is also necessary to design the structure of the transformer insulation.

6. Experimental Results and Comment

Realization of the Experimental Device

The realization of our solar regulator was carried out in the electrical engineering laboratory of the University Institute of Technology

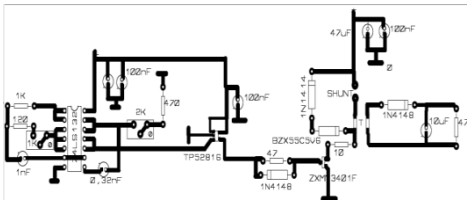

Practical realization of the device on the printed plate

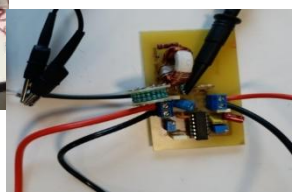

Electrical circuit Model assembly Model connection

Continuous Conduction Measurements at 205KHZ

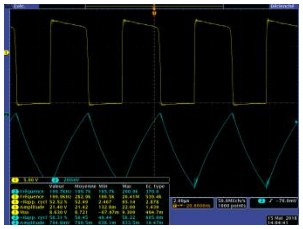

Mesures en conduction continue i0 non nul

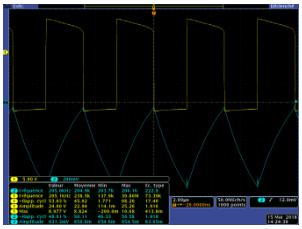

Comparaison tension mesurée et tension simulée

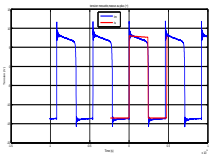

Comparaison courant mesuré et courant simulé

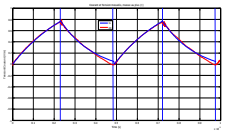

Comparaison courant mesuré et courant simulé (I0 non nul)

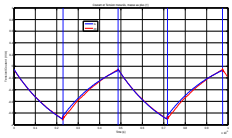

Mesures en conduction discontinue à 200khz

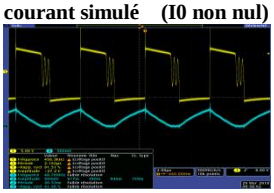

Shunt 5x5 ohm D 3cm 200khz

Continuous Conduction Measurements at 200KHZ

Comparison of the measurements according to the number of resistors forming the shunt from diameter 1.5cm to 200khz

Continuous Conduction Measurements at 200 KHZ

Comparison of the measurements according to the number of resistors forming the shunt from diameter 1.5cm to 200khz

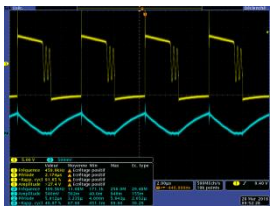

Shunt 10x 10ohm D 3cm 200khz

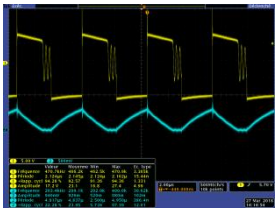

Shunt 20x 20ohm D 3cm 200khz

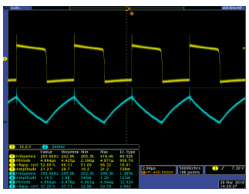

Shunt 5x5 ohm D 1,5cm 200khz

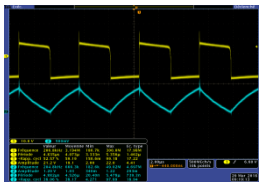

Shunt 10x10 ohm D 1,5cm 200khz (ancien shunt

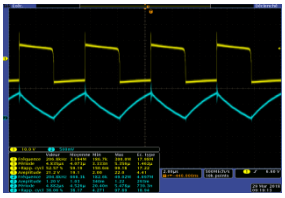

10x10 1,5cm ancien

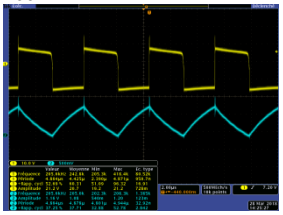

Shunt 5x5 ohms D 2cm

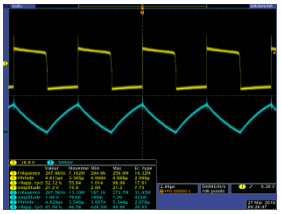

20x20 2c

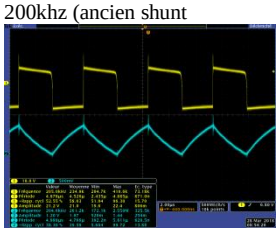

10x10 2cm

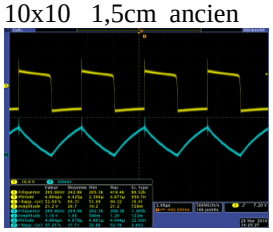

5x5 2cm

- Conclusion for the measurements according to the number of resistors forming the shunt with a diameter of two centimeters (2cm) at 200 kHz

  On the 3 oscillograms we note:

  a slight disturbance when switching the Mosfet from the non-passing state to the passing state but the 20 ohm shunt presents the best result.

  A disturbance during the switching of the Mosfet from the passing state to the non-passing state.

  In conclusion we can say the results obtained for the three measurements are almost similar

Comparison of measurements according to the number of resistors forming the shunt
Diameter three centimeters (3cm) at 200khz

Shunt 5x5ohms D 3cm 200khz

Shunt 10x10ohms D 3cm 200khz

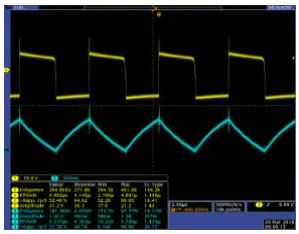

Shunt 20x20ohms D 3cm 200khz

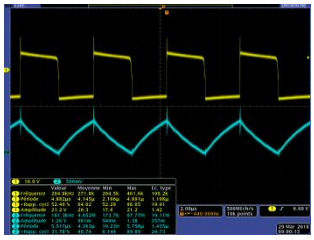

20x20 3cm

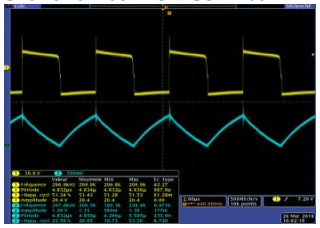

10x10 3cm

5x5 3cm

Conclusion for the measurements according to the number of resistors forming the shunt with a diameter of two centimeters (2cm) at 200 kHz.
On the 3 oscillograms we note:
a slight disturbance during the switching of the Mosfet from the non-passing state to the passing state of almost the same degree.
A disturbance during the switching of the Mosfet from the passing state to the non-passing state.
In conclusion we can say the results obtained for the three measurements are almost similar
Comparison of measurements according to the number of resistors forming the shunt From diameter 1.5cm to 200 kHz Mid-point output

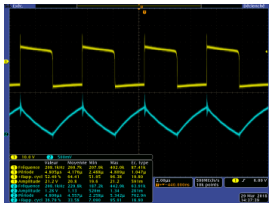

Shunt 10x10 D 2cm 200khz (ancien shunt) pt milieu

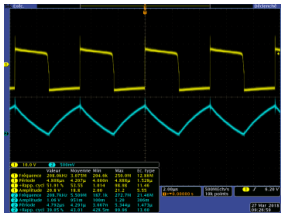

Shunt 20x20 D 2cm 200khz point milieu

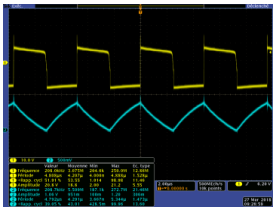

20x20 2cm

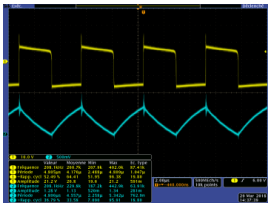

10x10 1,5cm

Conclusion for the measurements according to the number of resistors forming the shunt with a diameter of two centimeters (2cm) at 200 kHz.
On the 2 oscillograms we note:
a slight disturbance when switching the Mosfet from the non-passing state to the passing state but the 20 ohm shunt has the best result.
A disturbance during the switching of the Mosfet from the passing state to the non-passing state.
In conclusion we can say the results obtained for the three measurements are almost similar
Comparison of the measurements according to the point of taking of the shunt of diameter 2cm at 200khz
• Measurements Without Shunt 1ohm

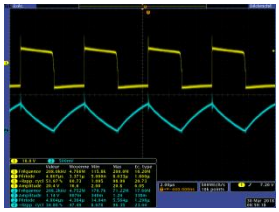

Mesures Sans Shunt 1ohm

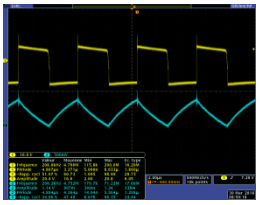

Shunt 5x5 ohms D 2cm

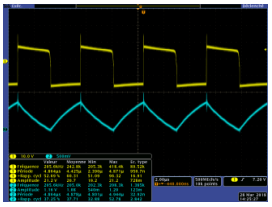

Shunt 10x10ohms D2cm 200khz

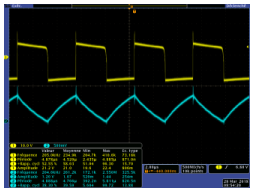

Shunt 20x20 ohm D2cm 200khz

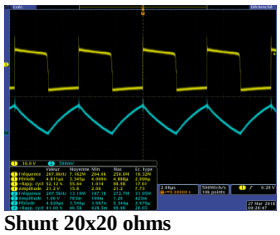

Shunt 20x20 ohms

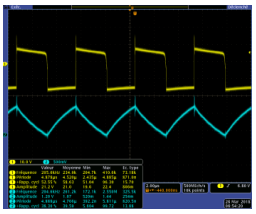

Shunt 5x5 2cm

Shunt 10x10 2cm

Shunt 20x20 2cm

Sans shunt

Conclusion for measurements without shunt and with shunts 5, 10, 20 ohms in diameter two centimeters (2cm) at 200khz

On the 4 oscillograms we note:

⎫ a slight disturbance during the switching of the Mosfet from the non-passing state to the passing state of almost the same degree for the 2 shunts of 5, 10 ohm and without shunt but the 20 ohm shunt presents a better result than these three measurements.

⎫ A disturbance during the switching of the Mosfet from the passing state to the non-passing state.

In conclusion we can say that among the results obtained the 20 ohm shunt has the best measurements but we note that the measurements without shunt are acceptable so when the measurements by shunt are necessary?

Comparison of measurements with shunt and without shunt at 500 kHz

Shunt 20x20 ohm D2cm

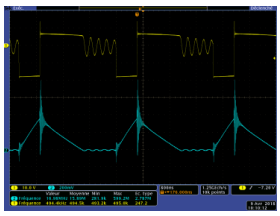

Résistance 1 ohm

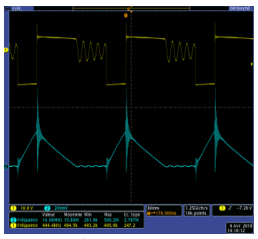

Résistance 1 ohm

Shunt 20x20

Conclusion for measurements with shunt and with the asselfic shunt 20x20 ohms in diameter two centimeters (2cm) at 500 kHz.

On the 2 oscillograms we note:

⎫ a disturbance when switching the Mosfet but the 20 ohm shunt presents a better result.

⎫ In conclusion we can say that among the results obtained the 20 ohm shunt has the best measurements than the no shun

References

[1]. Faouzi KAHLOUCHE, Fabrication et Caractérisation de MicroTransformateurs Planaires à Couches Magnétiques, Thèse de doctorat, UJM SAINT-ÉTIENNE, 10 juin 2014.

[2]. F. Kahlouche, K. Youssouf, M.H. Bechir, S. Capraro, A. Siblini, J.P. Chatelon, C. Buttay, J.J. Rousseau, « Fabrication and characterization of a planar interleaved micro-transformer with magnetic core », Microelectronics Journal Volume 45, Issue 7, July 2014, Pages 893–897

[3]. Y. Yamamoto, A. Makino, T. Yamaguchi, et I. Sasada, « Fine grained ferrite for low profile transformer », IEEE Trans. Magn., vol. 33, no 5, p. 3742‑3744, sept. 1997

[4]. Hurley, W.G.; Duffy, M.C. "Calculation of self- and mutual impedances in planar sandwich inductors" Magnetics, IEEE TransactionVolume 33, Issue 3, May 1997 Page(s):2282 - 2290

[5]. Jan Van Hese, "Tools and techniques for modelling spiral inductors on silicon", in Microwave Engineering, June 2002.

[6]. Y. Maycvskiy, « Analysis and Modeling of Monolithic On-Chip Transformers on Silicon Substrates », Thèse de Doctorat de l'Université Oregon, P-4, 2005.

[7]. S.S. Mohan, C.P. Yue, M. del Mar Hershenson, S.S. Wong, T.H. Lee, "Modeling and characterization of on- Chip transformers", Electron Devices Meeting, 1998. IEDM '98 Technisas Digest., International, 6-9 Dec. 1998 Page(s):531 – 534

[8]. J.C. Escamilla, P. Moreno, P. Gómez, "New model for overhead lossy multiconductor transmission lines," IET Generation, Transmission & Distribution, vol. 7, no. 11,